JOURNAL OF GEOPHYSICAL RESEARCH, VOL. 95, NO. A6, PAGES 8243–8251, JUNE 1, 1990

A Solar EUV Flux Model

W. KENT TOBISKA[1]

Cooperative Institute for Research in Environmental Sciences, National Oceanic and Atmospheric Administration University of Colorado, Boulder

CHARLES A. BARTH

Laboratory for Atmospheric and Space Physics, University of Colorado, Boulder

A model of the solar extreme ultraviolet (EUV) irradiance variability has been developed for aeronomical use and has been named SERF2 by the Solar Electromagnetic Radiation Flux Study. The model is valid between 1981 and 1989 and is based on the Atmosphere Explorer E (AE-E) satellite EUV data set which is correlated with independent solar emissions measured during and after the AE-E mission. Additionally, spectral modifications are made to the model based on 18 separate rocket flights for all levels of solar activity. Two daily measured solar emissions, the H Lyman α line at 121.6 nm observed by the Solar Mesosphere Explorer satellite and the Ottawa 10.7-cm radio flux observed at the ground, are used in the model as indices for full-disk solar EUV chromospheric irradiance variations and transition region–coronal irradiance variations, respectively. The model wavelength equation coefficients are presented in tabular form for 39 wavelength groups or discrete lines from 1.9 to 105.0 nm along with spectral weighting function coefficients which modify the irradiance magnitudes based upon model wavelength fits to rocket-observed spectra. The model satisfies the general constraint of duplicating rocket-observed EUV irradiance for a wide variety of solar activity conditions. The model development is discussed, an example calculation is given, and the comparisons with constraining rocket data sets are shown.

INTRODUCTION

The upper atmosphere of the Earth is of great interest to a number of scientific and engineering communities. The atmosphere's structure between 100 and 500 km varies in response to solar energy, auroral energy, and tides. The net result of photoabsorption, auroral particle precipitation, and Joule dissipation of ionospheric currents, tides, and atmospheric waves is atmospheric heating. The most significant component in global thermospheric heating is the introduction of energy from EUV and soft X ray wavelengths in the solar electromagnetic spectrum. This spectral range is created in the solar chromosphere, chromosphere-corona transition region, and corona. This flux, consisting of wavelengths shorter than 102.7 nm down to the X rays, is absorbed in the upper atmosphere by the major neutral constituents of O, N_2, and O_2. These emissions are also responsible for the ionization of the E and F regions, and their variation in time is one of the fundamental variables in thermospheric and ionospheric physics.

In the future, direct and instantaneous measurements of thermospheric density, composition, and temperature may become regularly available. However, until consistent monitoring can take place, modeling of the thermosphere will be the primary means of determining and predicting variations in the fundamental characteristics of temperature and density. The current problem of accurately modeling the density and temperature of the thermosphere as it varies with solar activity partially results from the lack of consistently measured solar EUV and soft X ray emissions.

Since EUV wavelengths are entirely absorbed prior to reaching the ground, the only methods of measuring them to the present have been rocket flights and satellite observations. These solar EUV measurements by satellites have been conducted on a daily basis during brief intervals of time: in the late 1960s by the OSO series satellites, in the early 1970s by the AEROS satellites, in the late 1970s by the Atmosphere Explorer (AE) series satellites, by Prognoz 10 in 1985, and by the San Marco satellite in 1988. Future observations may be made of the direct or indirect solar EUV irradiance variations by the absolute, extreme-ultraviolet, solar spectral irradiance monitor (AESSIM) instrument [*Huber et al.*, 1988], SOHO satellite [*Huber et al.*, 1988], and EUVE satellite [*Bowyer*, 1983; Extreme Ultra Violet Explorer Informational Package, Space Astrophysics Group, University of California, Berkeley, 1989]. This paucity of daily data, especially pronounced beginning in the 1980s, has been referred to as "the EUV hole" by *Donnelly* [1987*a*]. Therefore the EUV has mainly been parameterized by indices of solar activity which are observed at the Earth's surface. Zurich sunspot numbers, Rz, and 10.7-cm solar radio flux, $F_{10.7}$, have historically been used as indicators of the general level of solar EUV flux, although neither has any direct influence on the terrestrial atmosphere.

Previous empirical modeling of the solar EUV flux began prior to space-based observations with *Saha* [1937], who suggested an "ultraviolet excess factor" of up to 1×10^6 modification of the solar blackbody spectrum of 6500 K. After EUV measurements were made above the Earth's atmosphere, *Hinteregger et al.* [1965] tabulated what became known as an "EUV flux standard" based on rocket measurements, and *Roble and Schmidtke* [1979] identified typical examples of EUV flux during low and moderate solar

[1]Now at Space Sciences Laboratory, University of California, Berkeley.

Paper number 89JA03304.
0148-0227/90/89JA-03304$05.00

TABLE 1. Data Sets Used in Solar EUV Flux Model

Data Set	Time Period	Use in Model
AE-E Lyman α	July 1, 1977, to Dec. 21, 1978	linear correlation
AE-E EUV	July 1, 1977, to Dec. 21, 1978	linear correlation
$F_{10.7}$	July 1, 1977, to Dec. 21, 1978	linear correlation
$F_{10.7}$	Jan. 1, 1982, to Aug. 26, 1986	EUV flux index time series
SME Lyman α	Jan. 1, 1982, to Aug. 26, 1986	EUV flux index time series
LASP EUV rocket	Nov. 10, 1988 [*Woods and Rottman*, 1990]	weighting functions for $\lambda > 30.0$ nm
17 EUV rockets	all solar levels [*Feng et al.*, 1989]	weighting functions for $\lambda < 30.0$ nm

conditions for aeronomical applications. *Hinteregger et al.* [1981] developed empirical EUV flux models by using two modeling methods: (1) a two-variable $F_{10.7}$ association formula, using daily $F_{10.7}$ and its 81-day averaged and (2) an EUV class model. The $F_{10.7}$ association model is given for the EUV flux I at a wavelength λ:

$$I_\lambda = A_\lambda F^*_{10.7} + B_\lambda(F_{10.7} - F^*_{10.7}) + C_\lambda \quad \text{photons cm}^{-2}\ \text{s}^{-1} \tag{1}$$

where $F_{10.7}$ is the daily value and $F^*_{10.7}$ is the 81-day mean. A_λ, B_λ, and C_λ are obtained from a least squares fit to the AE-E EUV data. Equation (1) models the EUV flux for time periods other than those covered by the AE-E data set, is reviewed by *Schmidtke* [1984], is now called SERF1, and has been compiled in digital form by the Solar Electromagnetic Radiation Flux Study subgroup of the World Ionosphere-Thermosphere Study (WITS). WITS is an international interdisciplinary program of research organized by the Scientific Committee on Solar-Terrestrial Physics (SCOSTEP) which started July 1, 1987, and continued to December 31, 1989. SERF1 is available from the NOAA National Geophysical Data Center (NGDC).

However, a more accurate representation of EUV flux for the period during the AE-E mission is given by I_λ in the EUV class model,

$$I_\lambda = I_{\lambda\text{ref}} + I_{\lambda\text{ref}}(R_k - 1)C_\lambda \quad \text{photons cm}^{-2}\ \text{s}^{-1} \tag{2}$$

where $I_{\lambda\text{ref}}$ is the EUV flux at solar cycle 21 minimum given by *Hinteregger et al.* [1981]. R_k is the ratio for a specific date of a key EUV flux to the solar minimum value. C_λ is a wavelength-dependent scaling parameter for each EUV wavelength. The two key emissions are a chromospheric emission, Lyman β (102.6 nm), and a coronal emission, Fe XVI (33.5 nm). *Schmidtke* [1984] further reviews the EUV class model along with other methods of representing solar EUV flux for aeronomical applications. Previous work [*Hinteregger et al.*, 1981; *Bossy and Nicolet*, 1981; *Bossy*, 1983; *Hedin*, 1984; *Donnelly et al.*, 1986; *Tobiska and Barth*, 1988*a*] has shown that the AE-E EUV flux may be compared with the $F_{10.7}$. *Tobiska and Barth* [1988*a*] also compared the EUV flux to Lyman α and to the GOES 1- to 8-Å X rays. Conclusions from this body of work indicate that the greatest correlations in the AE-E data set are as follows: the chromospheric EUV emissions are most highly correlated with Lyman α, and the transition region–coronal emissions are most highly correlated with $F_{10.7}$.

This present work introduces solar Lyman α flux combined with $F_{10.7}$ as indices for the full-disk solar EUV irradiance variation. It follows the approach of *Hinteregger et al.* [1981] of estimating the full EUV spectrum using measurements of discrete lines which are created in similar solar source regions. The original indices from *Hinteregger et al.* [1981] of Lyman β and Fe XVI are no longer available on a daily basis. *Tobiska* [1988] and *Tobiska and Barth* [1988*a*] show that the solar Lyman α, measured on a daily basis by the Solar Mesosphere Explorer (SME) [*Rottman et al.*, 1982; *Rottman*, 1987] for $7\frac{1}{2}$ years (G. Rottman, private communication, 1989), and the $F_{10.7}$ emission, measured at the Ottawa observatory since 1947, are useful indices for modeling the dominant EUV and soft X ray emissions. Solar Lyman α is an effective chromospheric EUV emission indicator, and $F_{10.7}$ is an effective transition region and coronal EUV emission indicator. The EUV flux model based on this work has been named SERF2 by the Solar Electromagnetic Radiation Flux Study.

An overview of the modeling details can be summarized. AE-E Lyman α is linearly correlated with solar chromospheric region AE-E EUV flux, and $F_{10.7}$ is linearly correlated with solar transition region and coronal AE-E EUV flux such that least squares coefficients are obtained for the basic model at 39 wavelength intervals or discrete lines. Next, a constraint for the model to reproduce rocket-observed spectra for all levels of solar activity is placed on the model to improve its accuracy. This is accomplished by developing spectral weighting functions which are empirically determined and which enable a match between the model spectrum derived from the AE-E correlations and the spectrum observed by several rockets of discrete lines as well as broadband integrated flux. The complete EUV model is presented in tabular form for ease of use in aeronomical applications. The format of 39 wavelength intervals or discrete lines is the same as the 37 categories outlined by *Torr et al.* [1979] and *Torr and Torr* [1985] with the exception that two intervals in the soft X rays (1.9–3.0 nm and 3.0–4.9 nm) are added to the model.

SOLAR EUV MODEL

Data from five separate sources, comprising seven data sets and spanning over a decade between 1977 and 1988, are used in this study and shown in Table 1. Two particular satellites, the AE-E and SME, have made long-term observations of the solar spectrum and have provided data which are used in this work. Solar radio data from the World Data Center (WDC) are extensively used. Results from 18 EUV rocket flights [*Feng et al.*, 1989; *Woods and Rottman*, 1990] have also been incorporated into this model.

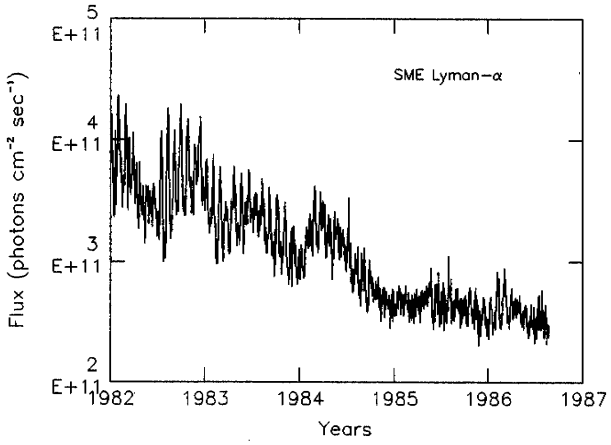

Fig. 1. Three-day smoothed daily averaged SME Lyman α between January 1, 1982, and August 26, 1986.

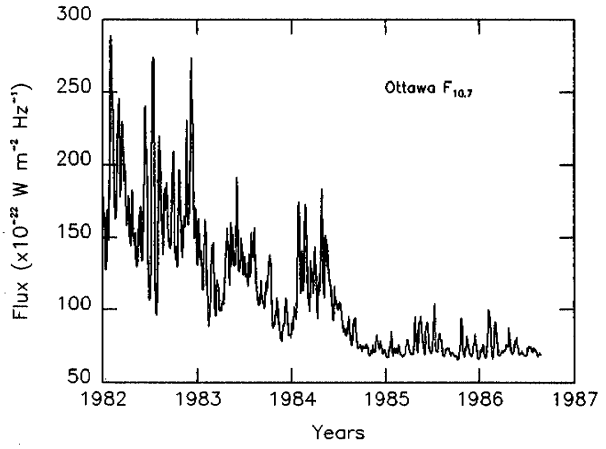

Fig. 2. Daily observed Ottawa 10.7-cm radio emission between January 1, 1982, and August 26, 1986.

Figures 1 and 2 show the model's two indices, SME Lyman α and the Ottawa $F_{10.7}$, for the period of time from January 1, 1982, through August 26, 1986. Both solar emissions show an underlying decline of flux intensity during the decline of cycle 21 to solar minimum with superimposed 27-day solar rotational variations and longer-period intermediate-term variations persisting for several solar rotations. The Lyman α daily minimum is in August 1986, and the $F_{10.7}$ daily minimum is in September 1986.

This model is based on the linear correlations of AE-E Lyman α with the AE-E chromospheric EUV emissions and of $F_{10.7}$ with the AE-E transition region–coronal emissions during the rise of cycle 21 from July 1, 1977, through December 21, 1978. The data during the rise of solar cycle 21 through December 21, 1978, were used in this study for two reasons. First, it was important to select a range of data which demonstrated considerable variation in magnitude in order to sample low, moderate, and high solar activity. Second, there is debate in the literature concerning the source of an apparent abrupt magnitude change of AE-E Lyman α after December 21, 1978 [*Bossy and Nicolet*, 1981; *Bossy*, 1983; *Fukui*, 1988]. Therefore, after December 21, 1978, AE-E Lyman α data were not used for this study.

The coefficients of linear correlation between the data sets for the period of the full AE-E mission (July 1, 1977, through December 30, 1980) have been summarized by *Hedin* [1984] and for the rise of cycle 21 by *Tobiska and Barth* [1988*a*]. These are summarized in Table 2. The important feature in Table 2 is that the Lyman α correlations are highest with the chromospheric EUV emissions and the $F_{10.7}$ correlations are highest with the transition region–coronal EUV emissions. There is a fairly good correlation between all comparisons, one might argue, but the coefficient of correlation has a substantial component which is likely to be influenced by the long-term trends in the data sets (O. R. White, private communication, 1988). For this study, the AE-E Lyman α and $F_{10.7}$ data are smoothed with a 13-day running mean algorithm to remove short-term variations. The smoothed data are then linearly correlated with each of the AE-E 39 wavelength intervals or discrete lines listed in Tables 3 and 4.

TABLE 2. Linear Correlation Coefficients for AE-E Data

Wavelength Interval, Å	Solar Source Region*	Correlation With Lyman α†	Correlation With $F_{10.7}$†	Correlation With $F_{10.7}$‡
168–190	T, CC	0.80	0.89	0.84
169–173	T	0.77	0.86	0.82
178–183	T, CC	0.80	0.87	0.84
190–206	T, CC	0.81	0.88	0.85
200–204	CC	0.82	0.88	0.85
206–255	Ch + BT, T, CC, HC	0.82	0.91	0.89
255–300	HC, Ch + BT	0.83	0.91	0.90
284	HC	0.85	0.92	0.91
304	Ch + BT	0.85	0.85	0.90
335	HC	0.82	0.95	0.94
510–580	Ch + T	0.89	0.83	0.86
584	Ch + BT	0.89	0.86	0.88
590–660	Ch, T, CC	0.88	0.83	0.85
1026	Ch + BT	0.91	0.89	0.90

*Code adapted from *Donnelly* [1987*b*]: Ch = chromosphere; BT = base of the transition region between the chromosphere and corona; T = chromosphere-corona transition region; CC = cool corona; HC = hot corona.

†From *Tobiska and Barth* [1988*a*] for the period July 1, 1977, through December 21, 1978.

‡From *Hedin* [1984] for the period July 1, 1977, through December 30, 1980.

TABLE 3. Chromospheric Emission Coefficients

Wavelength Interval	Intercept	Slope
18.62–29.52	0.0000E+00	0.0000E+00
30.02–49.22	8.64574E−04	9.60715E−04
50.52–99.99	9.16964E−03	1.01854E−02
100.54–148.40	2.44611E−03	2.36549E−03
150.10–198.58	9.83623E−03	3.80251E−03
200.02–249.18	1.15316E−02	4.47421E−03
256.32–256.32	1.15847E−02	1.65490E−03
284.15–284.15	0.0000E+00	0.0000E+00
251.10–299.50	1.74342E−04	9.66984E−04
303.31–303.31	0.0000E+00	0.0000E+00
303.78–303.78	2.49580E−01	3.56501E−02
303.31–349.85	0.0000E+00	0.0000E+00
368.07–368.07	0.0000E+00	0.0000E+00
356.01–399.82	4.32063E−04	9.68613E−05
401.14–436.70	4.47497E−03	1.00319E−03
465.22–465.22	0.0000E+00	0.0000E+00
453.00–499.37	1.88729E−03	1.78671E−03
500.00–550.00	7.18125E−03	2.78783E−03
554.37–554.37	1.56790E−02	3.23537E−03
584.33–584.33	1.50905E−03	1.30326E−02
554.37–599.60	6.98594E−03	2.30912E−03
609.76–609.76	0.0000E+00	0.0000E+00
629.73–629.73	2.53029E−02	5.49650E−03
609.76–644.10	1.18972E−03	3.45875E−04
650.30–700.00	2.01972E−03	6.84290E−04
703.36–703.36	6.54365E−03	1.12692E−03
701.00–750.00	8.78830E−04	8.35838E−04
765.15–765.15	2.22136E−03	7.39790E−04
770.41–770.41	0.0000E+00	0.0000E+00
787.71–787.71	3.83174E−03	7.90574E−04
750.01–800.00	1.23617E−02	4.91086E−03
801.00–850.00	9.98898E−03	9.10774E−03
851.00–900.00	1.63340E−03	2.46990E−02
901.00–950.00	7.98482E−03	2.06026E−02
977.02–977.02	4.86867E−02	1.80840E−02
951.00–1000.00	1.00441E−02	6.61423E−03
1025.70–1025.70	1.37646E−03	2.08082E−02
1031.90–1031.90	−1.47633E−03	1.56699E−02
1001.00–1050.00	1.82233E−02	1.30975E−02

Intercept and slope coefficients in the equation $E_\lambda = a + bw_{chr}$(Lyman α) where SME Lyman α is in ergs per square centimeter per second and is smoothed with a 13-day running mean algorithm. Read 8.64574E−04 as 8.64574×10^{-4}.

The 39 wavelength intervals or discrete lines are formed in the following manner. Each of the several hundred lines in the spectral range of 1.9–105.0 nm is classified as chromospheric or transition region–coronal in origin according to the *Hinteregger et al.* [1981] method of key = 1 or key = 2, respectively, used in the AE-E EUV solar minimum reference spectrum SC#21REFW. The full range of EUV lines are recreated in a time series from the method summarized in equation (2) above. The line intensities are summed to form intensities integrated over an interval where necessary. In cases where discrete lines are listed separately in Tables 3 and 4, these lines are not included in the intervals. The EUV calculated irradiance time series from equation (2) are then smoothed with the 13-day running mean, and a correlation is performed with either AE-E Lyman α or $F_{10.7}$ depending upon their chromospheric or transition region–coronal origin, respectively. The resulting intercept and slope coefficients are listed in Tables 3 and 4 for the chromospheric and transition region–coronal energy flux.

After the wavelength coefficients are obtained from the AE-E data comparisons, the model is next extended to the post–AE-E period. SME Lyman α and $F_{10.7}$ from 1981–1989 are used to do this. In order to create EUV flux which is representative of given solar conditions for time periods beyond the correlation time interval, the chromospheric and transition region–coronal energy flux time series are first created from the coefficients in Tables 3 and 4 using the input indices of 13-day smoothed SME Lyman α or $F_{10.7}$, respectively. Then the modeled EUV flux is modified with spectral weighting functions which have been empirically determined to adjust the model results at each wavelength to the observed EUV flux by rocket flights. These functions, w_1, w_2, and w_{chr}, enable the model to spectrally match the November 10, 1988, Laboratory for Atmospheric and Space Physics (LASP) EUV rocket flight [*Woods and Rottman*, 1990] and spectrally approximate the integrated soft X ray and EUV flux from 17 rocket flights during diverse solar activity conditions which are reviewed by *Feng et al.* [1989]. The empirically determined weighting functions are applied to the calculations of the chromospheric and transition region–coronal energy fluxes separately before summing both components into a full-disk modeled interval flux.

The chromospheric energy flux is calculated and modified by

TABLE 4. Transition Region and Coronal Emission Coefficients

Wavelength Interval	Intercept	Slope
18.62–29.52	−1.79720E−02	3.18809E−04
30.02–49.22	−1.77202E−02	3.40050E−04
50.52–99.99	−6.42898E−03	7.99157E−04
100.54–148.40	3.26442E−03	8.74992E−05
150.10–198.58	1.27261E−02	2.38466E−03
200.02–249.18	−5.92997E−02	1.54553E−03
256.32–256.32	0.0000E+00	0.0000E+00
284.15–284.15	−9.36616E−02	1.39477E−03
251.10–299.50	−6.51540E−02	1.70927E−03
303.31–303.31	−4.97807E−02	9.03115E−04
303.78–303.78	0.0000E+00	0.0000E+00
303.31–349.85	−7.40308E−02	1.74077E−03
368.07–368.07	2.58679E−02	2.05401E−04
356.01–399.82	−3.80497E−02	6.45189E−04
401.14–436.70	8.15105E−04	1.29010E−04
465.22–465.22	4.49212E−03	4.58682E−05
453.00–499.37	−1.42005E−02	2.37533E−04
500.00–550.00	−5.78278E−03	9.88009E−05
554.37–554.37	0.0000E+00	0.0000E+00
584.33–584.33	0.0000E+00	0.0000E+00
554.37–599.60	0.0000E+00	0.0000E+00
609.76–609.76	1.72306E−04	2.00784E−04
629.73–629.73	0.0000E+00	0.0000E+00
609.76–644.10	−5.26566E−04	4.56454E−05
650.30–700.00	1.32153E−03	7.12330E−06
703.36–703.36	0.0000E+00	0.0000E+00
701.00–750.00	0.0000E+00	0.0000E+00
765.15–765.15	0.0000E+00	0.0000E+00
770.41–770.41	1.39946E−03	6.72645E−05
787.71–787.71	0.0000E+00	0.0000E+00
750.01–800.00	7.40834E−04	3.56129E−05
801.00–850.00	0.0000E+00	0.0000E+00
851.00–900.00	0.0000E+00	0.0000E+00
901.00–950.00	0.0000E+00	0.0000E+00
977.02–977.02	0.0000E+00	0.0000E+00
951.00–1000.00	0.0000E+00	0.0000E+00
1025.70–1025.70	0.0000E+00	0.0000E+00
1031.90–1031.90	0.0000E+00	0.0000E+00
1001.00–1050.00	0.0000E+00	0.0000E+00

Intercept and slope coefficients in the equation $E_\lambda = a + b(w_1 F_{10.7mod} + w_2 F_{10.7})$ where $F_{10.7}$ is in $\times 10^{-22}$ W m^{-2} Hz^{-1} and is smoothed with a 13-day running mean algorithm. Read −1.79720E−02 as -1.79720×10^{-2}.

TABLE 5. Weighting Values for EUV Emissions

Wavelength Interval	w_1	w_2	w_{chr}
18.62–29.52	0.00000	2.00000	1.0000
30.02–49.22	0.24000	1.76000	1.0000
50.52–99.99	0.80000	1.20000	1.0000
100.54–148.40	1.12500	1.12500	1.0000
150.10–198.58	1.12500	1.12500	1.0000
200.02–249.18	0.33750	1.91250	1.0000
256.32–256.32	0.00000	0.00000	1.0000
284.15–284.15	0.00000	1.05000	1.0000
251.10–299.50	0.18000	2.07000	1.0000
303.31–303.31	0.00000	1.17450	1.0000
303.78–303.78	0.00000	0.00000	0.5873
303.31–349.85	0.00000	1.38080	1.7260
368.07–368.07	0.00000	0.01272	0.0254
356.01–399.82	0.02037	1.20180	1.0184
401.14–436.70	0.24172	0.44890	3.4531
465.22–465.22	0.00000	1.04710	0.8055
453.00–499.37	0.29122	0.65524	0.7281
500.00–550.00	1.23810	0.56275	2.2510
554.37–554.37	0.00000	0.00000	0.5841
584.33–584.33	0.00000	0.00000	0.5258
554.37–599.60	0.00000	0.00000	1.6545
609.76–609.76	0.00000	0.42239	0.5280
629.73–629.73	0.00000	0.00000	0.6448
609.76–644.10	5.40850	3.60570	1.2019
650.30–700.00	2.22570	0.74191	2.4730
703.36–703.36	0.00000	0.00000	0.8529
701.00–750.00	0.00000	0.00000	2.8459
765.15–765.15	0.00000	0.00000	2.8179
770.41–770.41	0.00000	1.80570	1.2038
787.71–787.71	0.00000	0.00000	10.930
750.01–800.00	0.00000	0.00000	0.0000
801.00–850.00	0.00000	0.00000	1.9197
851.00–900.00	0.00000	0.00000	1.5441
901.00–950.00	0.00000	0.00000	1.5157
977.02–977.02	0.00000	0.00000	1.0000
951.00–1000.00	0.00000	0.00000	0.9826
1025.70–1025.70	0.00000	0.00000	1.0737
1031.90–1031.90	0.00000	0.00000	2.0631
1001.00–1050.00	0.00000	0.00000	0.0497

$$E_{\lambda chr} = a_1 + b_1 w_{chr} F_{Ly\alpha} \quad \text{ergs cm}^{-2}\ \text{s}^{-1} \tag{3}$$

where the subscript 1 refers to the intercept and slope coefficients in Table 3, $F_{Ly\alpha}$ is the 13-day smoothed SME Lyman α flux in ergs per square centimeter per second, and w_{chr} is a wavelength-dependent chromospheric weighting function whose values for each of the 39 wavelength intervals are listed in Table 5, last column. The average value of w_{chr} across all wavelengths, $\overline{w_{chr}} = 1.46$, corresponds to the approximate factor by which the solar minimum SME Lyman α must be multiplied in order to raise it to the AE-E Lyman α solar minimum value. Solar cycle 20 minimum (July 1976) for AE-E Lyman α is 3×10^{11} photons cm^{-2} s^{-1}, while solar cycle 21 minimum (August 1986) for SME Lyman α is 2.3×10^{11} photons cm^{-2} s^{-1}. This does not judge the AE-E nor the SME Lyman α calibrations. However, since the model correlations were made with the AE-E Lyman α data, the SME Lyman α should be scaled to the approximate AE-E values for modeling purposes. The w_{chr} function accomplishes this goal across the entire EUV spectrum along with allowing a spectral line fit between the model and the rocket data. w_{chr} is derived using an iterative technique. This technique computationally converges to a weighting value for the modeled chromospheric flux in each interval or at each line such that there is less than 1% difference between the final model 5.0-nm bin value and the November 10, 1988, LASP rocket 5.0-nm bin value where the model uses the $F_{10.7}$ and Lyman α on that date for the initial flux calculation.

The transition region–coronal energy flux is calculated and modified by

$$E_{\lambda cor} = a_2 + b_2(w_1 F_{10.7mod} + w_2 F_{10.7}) \quad \text{ergs cm}^{-2}\ \text{s}^{-1} \tag{4}$$

where the subscript 2 refers to the intercept and slope coefficients in Table 4. w_1 and w_2 are wavelength-dependent transition region–coronal weighting functions whose values for each of the 39 wavelength intervals are listed in Table 5, second and third columns, respectively; w_1 and w_2 are empirically determined in a manner similar to that used for w_{chr}. $F_{10.7}$ in this equation is the 13-day smoothed $F_{10.7}$ value while $F_{10.7mod}$ is a pseudo-$F_{10.7}$ based upon the SME daily average Lyman α value correlated to $F_{10.7}$ during the decline of solar cycle 21. Here

$$F_{10.7mod} = -218.88 + 1.05453 \times 10^{-9}\text{Lyman } \alpha \tag{5}$$

where Lyman α in (5) is in photons cm^{-2} s^{-1}. $F_{10.7mod}$, as given in (5), is used both as an abbreviation within (4) and for empirical reasons. The latter reason is based on the assumption that there is a transition region component to $F_{10.7}$ that varies somewhat differently from the observed flux which comes from several source regions but which is strongly influenced by coronal emission. The $F_{10.7}$ index is split into two components, $F_{10.7mod}$ and $F_{10.7}$, in order to empirically weight the transition region–coronal flux with a temporal variation which has some similarity to chromospheric variations. This motivation is further discussed below.

The chromospheric and transition region–coronal components are both summed to give a total full-disk energy flux for that wavelength interval or discrete line from the method

$$E_\lambda = E_{\lambda chr} + E_{\lambda cor} \quad \text{ergs cm}^{-2}\ \text{s}^{-1} \tag{6}$$

This constitutes the solar EUV flux model.

An example of the model calculation of an EUV flux for given solar activity is as follows. If $F_{10.7} = 158.2 \times 10^{-22}$ W m^{-2} Hz^{-1} and Lyman $\alpha = 5.9 \times 10^{11}$ photons cm^{-2} s^{-1}, the energy flux for the mixed wavelength interval between 200.02 and 249.28 Å can be determined. The chromospheric energy fluxes from (3) in the interval are

$$E_{200-249chr} = 1.15316 \times 10^{-2} + (4.47421 \times 10^{-3})(1.0)(9.6421)$$
$$= 5.4672 \times 10^{-2} \quad \text{ergs cm}^{-2}\ \text{s}^{-1}$$

where

$$9.6421 = \frac{(5.9 \times 10^{11})(12{,}400)(1.602192 \times 10^{-12})}{1215.67}$$

is the conversion of Lyman α photon flux to energy flux. The transition region–coronal energy fluxes from (4) in the interval are

$$E_{200-249cor} = -5.92997 \times 10^{-2} + (1.54553 \times 10^{-3})[(0.3375)$$
$$\cdot(403.29) + (1.9125)(158.20)] = 0.6187 \quad \text{ergs cm}^{-2}\ \text{s}^{-1}$$

where

$$403.29 = -218.88 + (1.05453 \times 10^{-9})(5.9 \times 10^{11})$$

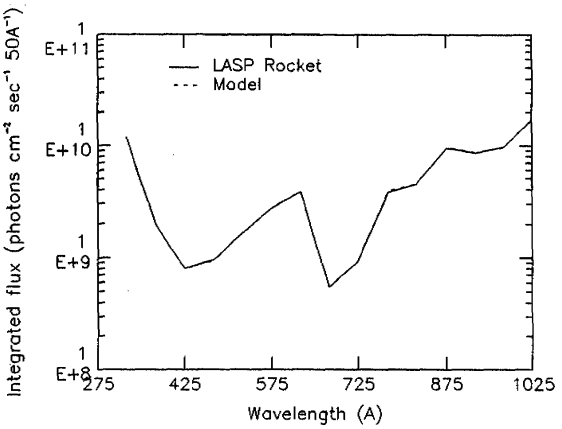

Fig. 3. LASP EUV rocket measurements (solid line) compared to the EUV model (dotted line) integrated over 5.0-nm intervals. The LASP rocket was launched from White Sands, New Mexico, on November 10, 1988. The EUV model is calculated with an SME Lyman $\alpha = 3.47 \times 10^{11}$ photons cm^{-2} s^{-1} and $F_{10.7} = 147.7 \times 10^{-22}$ W m^{-2} Hz^{-1} for this date. The weighting functions enable a match between the rocket data and model above 30.0 nm. *Woods and Rottman* [1990] give a derived Lyman α value of $3.30 \pm 0.5 \times 10^{11}$ photons cm^{-2} s^{-1} for the NO ionization cell on the same rocket flight and $3.35 \pm 0.3 \times 10^{11}$ photons cm^{-2} s^{-1} for SME. The SME Lyman α value of 3.47×10^{11} photons cm^{-2} s^{-1} used in the model calculation was taken from an earlier version of the SME data set (G. Rottman, private communication, 1989) and is within the error bars of the new values. The model EUV values are not independent of the LASP rocket data, and this figure serves to demonstrate the fit of the model to the data.

is the $F_{10.7mod}$ value. Thus the total integrated flux in these solar conditions for the wavelengths between 200.02 and 249.18 Å is

$$E_{200-249} = 0.0547 + 0.6187 = 0.6733 \quad \text{ergs cm}^{-2}\ \text{s}^{-1}$$

DISCUSSION

The particular constraint which this model must satisfy in order to provide credible EUV spectral intensities for any given solar activity is a reproduction of observed rocket spectra within the specified error bars. The comparison of model results with EUV data from rocket flights during a variety of levels of solar activity is discussed.

Woods and Rottman [1990] measured the solar EUV spectrum between 30.5 and 109.5 nm with a LASP sounding rocket experiment on November 10, 1988, which was launched at White Sands Missile Range, New Mexico. The published uncertainty in the 5-nm bin data ranges between 7 and 35%, is wavelength dependent, and has an overall average of 13% uncertainty. Figure 3 is the spectrum obtained by Woods and Rottman represented as 5.0-nm-binned data with the solid line. Overplotted on Figure 3 with a dotted line is the model EUV flux for this date based on the algorithm described above. This figure verifies an excellent reproduction of the LASP rocket data by the modeled flux for the 5.0-nm integrated flux intervals. This match results, of course, from using the LASP rocket data to spectrally constrain the model flux while deriving the spectral weighting functions described above and detailed in Figure 4. The w_{chr} function (solid line) in Figure 4 is constant in time, has a maximum value of 10.93, and has a minimum value of 0.0. It is used to modify the chromospheric line and interval intensities calculated from the Lyman α index in (3). If one were to use the average value of w_{chr} for the whole spectrum, it would be numerically approximate to increasing the values of SME Lyman α to those of AE-E during solar minimum, i.e., between 30 and 46%. Figure 4 also represents the spectral modifications required of the model due to the combined calibration and line fit differences between AE-E and rocket EUV data sets.

The summed w_1 and w_2 weighting functions in Figure 4, which modify the transition region–coronal line and interval intensities in (4), have an average value near 2 as well as a maximum of 9.01 and a minimum of 0.0 above 30.0 nm. Below 30.0 nm they have a maximum of 2.5 and a minimum of 1.05. These weights are based upon empirically determined best fits between the modeled EUV flux and the *Woods and Rottman* [1990] rocket data and between the modeled EUV flux and the *Feng et al.* [1989] rocket data in the ranges above 30.0 nm and below 30.0 nm, respectively. w_1 weights the $F_{10.7mod}$ term, which is based on a $F_{10.7}$ fit to Lyman α; w_2 weights the $F_{10.7}$ term. The approach of using a two-component $F_{10.7}$ index is motivated from the observation that the June 1982 satellite-derived density data at the top of the thermosphere [*Tobiska*, 1988; *Tobiska and Barth*, 1988*b*], which varies with EUV input, follow a chromospheric-type variation instead of a coronal-type temporal change. This two-component $F_{10.7}$ term allows for a slightly better modeled density representation during periods such as June 1982 based on an input modeled EUV irradiance variation. The relative time series variation of $F_{10.7mod}$ will be similar to that of Lyman α.

There have been numerous rocket flights since the late 1960s which have measured soft X ray and EUV irradiances. *Feng et al.* [1989] have reviewed the observations of these rocket experiments and have shown a composite reference

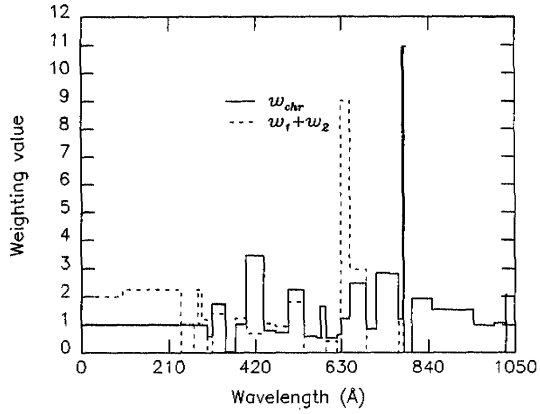

Fig. 4. Three spectral weighting functions w_{chr}, w_1, and w_2. The uses of these functions are described in the text. The weighting value represents a factor by which a model wavelength term is multiplied in order to achieve spectral consistency between a variety of EUV rocket measurements for diverse levels of solar activity. $w_1 + w_2$ is used to produce a summed term in equation (4). The abnormally large weight for w_{chr} shortward of 875 Å is a result of the fits for two discrete lines (765.15 Å = 2.82 and 787.71 Å = 10.93). The abnormally large weight for $w_1 + w_2$ results from a fit to the coronal component of the 600- to 650-Å interval (sum=9.01). $w_1 + w_2$ is generally a value of 2 based upon fits to both the *Feng et al.* [1989] integrated flux and the LASP rocket data.

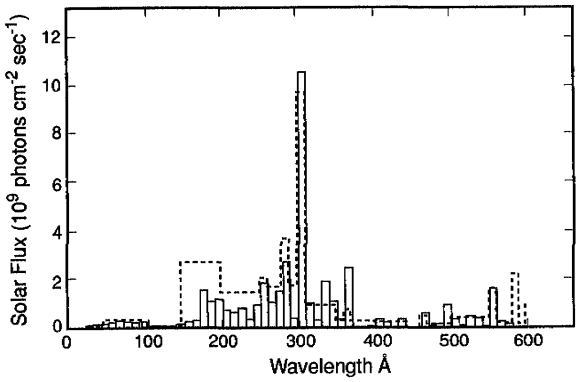

Fig. 5. The composite solar flux reference spectrum (solid line) is taken from *Feng et al.* [1989] and above 75 Å represents the AFGL rocket flight data of August 14, 1979, in 1.0-nm bins. The model (dotted line) consists of 5.0-nm-binned data averaged into 1.0-nm bins for the wavelength intervals listed in Tables 3, 4, and 5 while the discrete line modeled flux from these same tables is added into the appropriate 1.0-nm bin. The model spectrum was created with Lyman $\alpha = 5.9 \times 10^{11}$ photons cm^{-2} s^{-1} and $F_{10.7} = 158.2 \times 10^{-22}$ W m^{-2} Hz^{-1}.

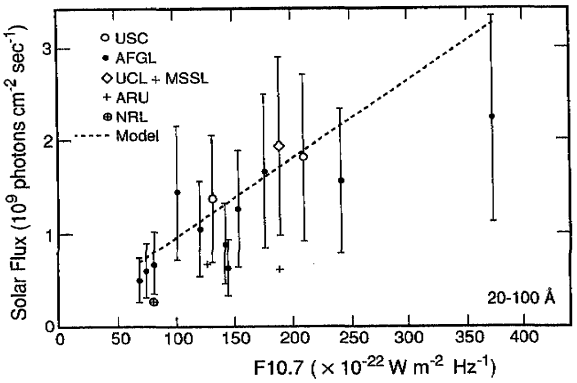

Fig. 6. The integrated solar soft X ray flux between 2.0 and 10.0 nm is taken from *Feng et al.* [1989] (points with error bars). These measurements are from rocket experiments performed by several organizations over a wide range of solar activity with $F_{10.7}$ ranging from 70 to 370. The EUV model estimated flux is shown as the dotted line and is described in the text. The acronyms are USC (University of Southern California), AFGL (Air Force Geophysics Laboratory), UCL (University College London), MSSL (Mullard Space Science Laboratory), ARU (Astrophysics Research Unit at Culham, England), and NRL (Naval Research Laboratory). From Feng et al., all error bars on the measurements are ±50%. The NRL and ARU photographic data have no error bars plotted.

spectrum as well as the integrated flux spectrum for 2.0–10.0 nm and 5.0–57.5 nm for low to high solar activity conditions. Figure 5 shows the Feng et al. composite spectrum as a solid line which is partially based upon the Air Force Geophysics Laboratory (AFGL) rocket experiment on August 14, 1979. The flux in $\times 10^9$ photons cm^{-2} s^{-1} is binned in 1.0-nm intervals. The modeled EUV flux has 5.0-nm bin resolution for each of the wavelength intervals but displayed in 1.0-nm bins where each wavelength interval bin is 20% of the 5-nm bin except for the contribution of discrete lines. The model values are shown as a dotted line in this composite spectrum. In Figure 5, $F_{10.7} = 158.2 \times 10^{-22}$ W m^{-2} Hz^{-1} from the NGDC, and Lyman $\alpha = 5.9 \times 10^{11}$ photons cm^{-2} s^{-1}. The Lyman α value was determined by reducing the AE-E Lyman α observed value of 7.7×10^{11} photons cm^{-2} s^{-1} by the ratio of AE-E to SME for solar minimum (1.3:1). This new Lyman α value is called an equivalent SME Lyman α value. The w_{chr} weighting function then restores the full weighting to the calculated chromospheric flux when used with the equivalent Lyman α. There is fairly good agreement with the important He II (30.4 nm) line as well as most other intervals and discrete lines in this composite spectrum. The apparent exceptions are the disagreements with the 15.0- to 20.0-nm and 20.0- to 25.0-nm intervals and the 36.8-nm line where the model is higher than the Feng et al. spectrum. Possible reasons for this disagreement are summarized below in the discussion on model weaknesses.

Figure 6 shows the Feng et al. 2.0- to 10.0-nm integrated spectrum for 17 rocket experiments from low to high solar activity denoted by $F_{10.7}$ from 70 to 370. The different symbols refer to rocket experiments by separate organizations. The dotted line is the interpolated flux values for seven cases of solar activity where the model was run with $F_{10.7}$ inputs of 70, 120, 170, 220, 270, 320, and 370. Lyman α inputs were 2.7×10^{11}, 3.2×10^{11}, 3.7×10^{11}, 4.2×10^{11}, 4.6×10^{11}, 5.1×10^{11}, and 5.6×10^{11}, respectively, which correspond to the approximate SME Lyman α values derived from the relationship in (5) using the seven $F_{10.7}$ values. The reader is reminded that the w_{chr} weighting function scales the SME Lyman α values to the approximate AE-E Lyman α values. These example cases were also calculated based on the assumption that Lyman α follows the same relative variation relationship to $F_{10.7}$ in August 1979 as it does between July 1977 and December 1978. The model is within the error bars for 13 out of 14 rocket measurements (there are no error bars for three rockets which made photographic observations).

Figure 7 shows the Feng et al. integrated spectrum for 5.0–57.5 nm in the same format as Figure 6. The modeled integrated EUV flux between 5.0 and 58.0 nm is overplotted. The model is within the error bars of 9 out of 14 rocket flights and is very close to one of the University of Southern

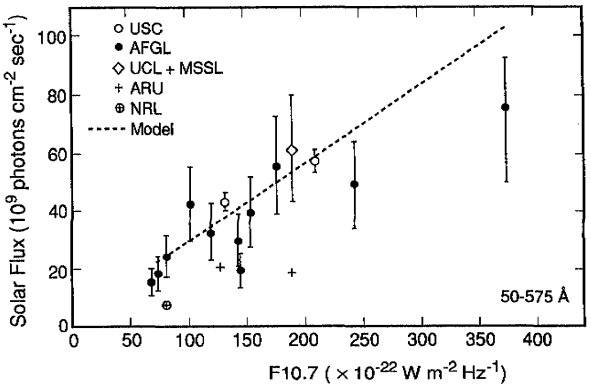

Fig. 7. The integrated solar EUV flux between 5.0 and 57.5 nm is taken from *Feng et al.* [1989] (points with error bars). The measurements are taken by the same organizations listed in the caption for Figure 6. The EUV model is represented as a dotted line and is described in the text. From Feng et al., all error bars on the measurements are ±30% except for the USC data, which are ±7%. The NRL and ARU photographic data have no error bars plotted.

California (USC) rockets with small uncertainty when $F_{10.7}$ was near 210.

It should be noted that the model, as initially calculated with only the AE-E derived coefficients in Tables 3 and 4, does not explicitly include continuum emission in the EUV since it is based upon correlations with the discrete lines in SC#21REFW. However, after the model is improved using the rocket-derived spectral weighting functions, the continuum is accounted for since both the Feng et al. and the Woods and Rottman data include continuum as well as discrete lines.

While the model delivers good results of solar EUV irradiance variation for all solar conditions, and especially for moderate solar activity, a summary of the model weaknesses is also appropriate. First, a comment should be made about the error in the model flux values. Absolute error is not quantified in this model since there are far too many variables in the seven data sets, each with several types of uncertainty, which prevents a reasonable analysis. However, the comparison of the model to the Feng et al. and Woods and Rottman results, while not an independent test of model accuracy, does give a qualitative view of the model uncertainty compared to the error bars of rocket observations. Figures 3, 5, 6, and 7 are useful for this type of comparison and have been discussed above.

Aside from the generally good EUV flux results, the model may still yield energy flux values which are too low for the total integrated flux between 5.0 and 57.5 nm during low solar activity and too high during high solar activity. This is based on an assessment of the data in Figure 7. If one were to draw a line through the two USC measurements in Figure 7, which have the smallest error bars, the above conclusion would be reached. The topic of low rocket measurements of EUV flux during low solar activity continues to be addressed in the literature by *Richards and Torr* [1984], *Ogawa and Judge* [1986], *Link et al.* [1988], and *Tobiska* [1989]. These authors would increase the solar minimum EUV below 25.0 nm by factors of 2.0, 2.0, 2.0, and 1.6, respectively, from the values shown in Figure 7. The latter value (1.6) is based upon this model's increase of the 15.0- to 25.0-nm integrated range value by 1.6 compared to the April 23, 1974, rocket spectrum (F74113) [*Hinteregger*, 1976; *Heroux and Hinteregger*, 1978], which was used to help calibrate the AE-C and AE-E satellite EUV instruments.

A comparison of the modeled EUV flux without using the weighting functions [*Tobiska*, 1990] shows a good correlation with the AE-E data sets. However, the correlation with AE-E data using the spectral weighting functions has yet to be evaluated.

CONCLUSIONS

A full-disk EUV and soft X ray flux model has been developed for the period of late 1981 into 1989. This corresponds to the declining and minimum phase of solar cycle 21 and the rising to maximum phase of solar cycle 22. The model calculates 39 wavelength intervals or prominent discrete lines between 1.9 and 105.0 nm in both magnitude and relative temporal variation. The model wavelength equations are based upon two 13-day smoothed solar indices, SME Lyman α and Ottawa $F_{10.7}$, which are used with tabulated coefficients and spectral weighting functions to produce both chromospheric and transition region–coronal energy fluxes. These are then summed to provide a total full-disk daily spectral energy flux.

The model is an advance over the SERF1 model, which is solely dependent upon the $F_{10.7}$ daily and 81-day values and thus uses a single mixed solar source region index to parameterize all EUV irradiances, regardless of source region. It builds upon the method of a previous EUV class model which associates EUV irradiances with an appropriate index based upon similar solar source region and a high correlation coefficient. While the EUV class model is appropriate for the time period of 1977–1980, the indices used in that model are no longer available after the end of the AE-E mission. For the post–AE-E EUV model, SERF2, there are solar index data (Lyman α and $F_{10.7}$) available for seven full years from late 1981 into 1989.

The principal use of this model is for aeronomical applications in order to calculate the EUV and soft X ray energy flux at the top of the atmosphere. A particular application of these energy fluxes will be to determine the amount of solar energy available for thermospheric heating during campaign periods. A second application of the model will be to assist in the intercomparison of rocket- and satellite-measured EUV data. The model is available in digital form upon request and will be available from the NGDC in early 1990.

Acknowledgments. The SME Lyman α data provided by G. J. Rottman (CU/LASP) and the AE-E Lyman α and EUV data provided by H. E. Hinteregger (AFGL) have been invaluable data sets for this model development. The efforts of these investigators is deeply appreciated. T. Woods (CU/LASP) has provided EUV rocket data which have greatly aided the model's development. H. Ogawa (USC/SSC) has provided EUV and soft X ray integrated flux data which have been extremely useful. R. F. Donnelly (NOAA) and S. C. Solomon (HAO/NCAR) have provided many useful comments and critiques throughout the development of this model.

The Editor thanks H. S. Ogawa and D. G. Torr for their assistance in evaluating this paper.

REFERENCES

Bossy, L., Solar indices and solar U.V.-irradiances, *Planet. Space Sci.*, *31*, 977, 1983.

Bossy, L., and M. Nicolet, On the variability of Lyman-alpha with solar activity, *Planet. Space Sci.*, *29*, 907, 1981.

Bowyer, S., The Extreme Ultraviolet Explorer, *Adv. Space Res.*, *2*, 157, 1983.

Donnelly, R. F., Gaps between solar UV and EUV radiometry and atmospheric sciences, in *Solar Radiative Output Variation, Proceedings of a Workshop Held Nov. 9–11, 1987*, edited by P. Foukal, p. 139, National Center for Atmospheric Research, Boulder, Colo., 1987*a*.

Donnelly, R. F., Temporal trends of solar EUV and UV full-disk fluxes, *Sol. Phys.*, *109*, 37, 1987*b*.

Donnelly, R. F., H. E. Hinteregger, and D. F. Heath, Temporal variations of solar EUV, UV, and 10,830-Å radiations, *J. Geophys. Res.*, *91*, 5567, 1986.

Feng, W., H. S. Ogawa, and D. L. Judge, The absolute solar soft X ray flux in the 20–100 Å region, *J. Geophys. Res.*, *94*, 9125, 1989.

Fukui, K., Unique increase of solar Lyman alpha flux observed by AE-E satellite during cycle 21, *Eos Trans. AGU*, *69*, 417, 1988.

Hedin, A. E., Correlations between thermospheric density and temperature, solar EUV flux, and 10.7-cm flux variations, *J. Geophys. Res.*, *89*, 9828, 1984.

Heroux, L., and H. E. Hinteregger, Aeronomical reference spectrum for solar UV below 2000 Å, *J. Geophys. Res.*, *83*, 5305, 1978.

Hinteregger, H. E., EUV fluxes in the solar spectrum below 2000 Å, *J. Atmos. Terr. Phys.*, *38*, 791, 1976.

Hinteregger, H. E., L. A. Hall, and G. Schmidtke, Solar XUV radiation and neutral particle distribution in July 1963 thermosphere, *Space Res.*, *V*, 1175, 1965.

Hinteregger, H. E., K. Fukui, and B. R. Gilson, Observational, reference and model data on solar EUV, from measurements on AE-E, *Geophys. Res. Lett.*, *8*, 1147, 1981.

Huber, M. C. E., P. L. Smith, W. H. Parkinson, M. Kühne, and M. Kock, Absolute, extreme-ultraviolet, solar spectral irradiance monitor (AES-SIM), *Adv. Space Res.*, *8*, 81, 1988.

Link, R., G. R. Gladstone, S. Chakrabarti, and J. C. McConnell, A reanalysis of rocket measurements of the ultraviolet dayglow, *J. Geophys. Res.*, *93*, 14,631, 1988.

Ogawa, H. S., and D. L. Judge, Absolute solar flux measurement shortward of 575 Å, *J. Geophys. Res.*, *91*, 7089, 1986.

Richards, P. G., and D. G. Torr, An investigation of the consistency of the ionospheric measurements of the photoelectron flux and solar EUV flux, *J. Geophys. Res.*, *89*, 5625, 1984.

Roble, R. G., and G. Schmidtke, Calculated ionospheric variations due to changes in the solar EUV flux measured by the AEROS spacecraft, *J. Atmos. Terr. Phys.*, *41*, 153, 1979.

Rottman, G. J., Results from space measurements of solar UV and EUV flux, in *Solar Radiative Output Variation, Proceedings of a Workshop Held Nov. 9–11, 1987*, edited by P. Foukal, p. 71, National Center for Atmospheric Research, Boulder, Colo., 1987.

Rottman, G. J., C. A. Barth, R. J. Thomas, G. H. Mount, G. M. Lawrence, D. W. Rusch, R. W. Sanders, G. E. Thomas, and J. London, Solar spectral irradiance, 120 to 190 nm, *Geophys. Res. Lett.*, *9*, 587, 1982.

Saha, M. N., On the action of ultra-violet sunlight upon the upper atmosphere, *Proc. R. Soc. London, Ser. A*, *160*, 155, 1937.

Schmidtke, G., Modelling of the solar extreme ultraviolet irradiance for aeronomic applications, *Handb. Phys.*, *XLIX*(7), *Geophysics III, Part VII*, 1, 1984.

Tobiska, W. K., A solar extreme ultraviolet flux model, Ph.D. thesis, Dep. of Aerosp. Eng., Univ. of Colo., Boulder, 1988.

Tobiska, W. K., Modeled solar EUV flux during the Equinox Transition Study: September 17–24, 1984, *J. Geophys. Res.*, *94*, 17,017, 1989.

Tobiska, W. K., SERF2: A solar extreme ultraviolet flux model, *Earth Planet. Atmos. Group Contrib. 9*, Space Sci. Lab., Univ. of Calif., Berkeley, Jan. 1990.

Tobiska, W. K., and C. A. Barth, Comparison of solar indices for EUV fluxes, *Eos Trans. AGU*, *69*, 418, 1988*a*.

Tobiska, W. K., and C. A. Barth, A comparison of thermospheric models with parameterized EUV heating, *Eos Trans. AGU*, *69*, 1345, 1988*b*.

Torr, M. R., and D. G. Torr, Ionization frequencies for solar cycle 21: Revised, *J. Geophys. Res.*, *90*, 6675, 1985.

Torr, M. R., D. G. Torr, R. A. Ong, and H. E. Hinteregger, Ionization frequencies for major thermospheric constituents as a function of solar cycle 21, *Geophys. Res. Lett.*, *6*, 771, 1979.

Woods, T. N., and G. J. Rottman, Solar EUV irradiance derived from a sounding rocket experiment on November 10, 1988, *J. Geophys. Res.*, *95*, 6227, 1990.

C. A. Barth, Laboratory for Atmospheric and Space Physics, Campus Box 392, University of Colorado, Boulder, CO 80309.

W. K. Tobiska, Space Sciences Laboratory, University of California, Berkeley, CA 94720.

(Received June 19, 1989;
revised October 5, 1989;
accepted October 23, 1989.)